A Galinstan-Filled Capillary Probe for Thermal Conductivity Measurements and its Application to Molten Eutectic KNO_3-$NaNO_3$-NO_2 (HTS) up to 700 K

Niccolo Le Brun, Christos N. Markides[1,*]

Clean Energy Processes (CEP) Laboratory, Department of Chemical Engineering, Imperial College London, South Kensington Campus, London, SW7 2AZ, U.K.

Abstract

The successful measurement of the thermal conductivity of molten salts is a challenging undertaking due to the electrically conducting and possibly also aggressive nature of the materials, as well as the elevated temperatures at which these data are required. For accurate and reproducible measurements it is important to develop a suitable experimental apparatus and methodology. In this study we explore a modified version of the transient hot-wire method, which employs a molten-metal-filled capillary in order to circumvent some of the issues encountered in previous studies. Specifically, by using a novel flexible U-shaped quartz-capillary, filled with a eutectic mixture of gallium, indium and tin, commercially known as Galinstan, we proceed to measure the thermal conductivity of molten eutectic $KNO_3-NaNO_3-NaNO_2$. The new probe is demonstrated as being able to measure the thermal conductivity of this molten salt, which is found to range from 0.48 W/m K at 500 K to 0.47 W/m K at close to 700 K, with an overall expanded uncertainty (95% confidence) of 3.1%. The quartz is found to retain its electrically insulating properties and no current leakage is detected in the sample over the investigated temperature range. The thermal conductivity data reported in the present study are also used to elucidate a partial disagreement found in the literature for this material.

Keywords: thermal conductivity, molten salt, heat-transfer salt, transient hot-wire, metal-filled capillary

*Corresponding author

Email address: c.markides@imperial.ac.uk (Christos N. Markides)

[1]Telephone: +44 (0)20 7594 1601

1. Introduction

Molten salts are of particular interest in many applications related to the energy sector, and their employment is envisaged to experience a significant growth. Their thermophysical properties make them advantageous as heat transfer fluids, in next-generation nuclear-reactors, and in energy storage applications. As indicated by Nunes et al. [1], in order to fully exploit the potential of molten-salt materials it is essential to obtain reliable values of their thermophysical properties. Thermal conductivity data, in particular, are associated with large scatter and uncertainty even for the most common types of salts, owing to a number of difficulties involved in the relevant measurements. Most of the currently available data are still the result of the significant experimental efforts conducted between the 1960s and the 1980s. More recently, apart from a few exceptions, e.g. Zhang et al. [2], the experimental work conducted in this area seems to have stagnated. Given the renewed interest in these materials from an application perspective, and the acceleration in the formulation of suitable materials, it is important to renew the experimental efforts towards the determination of their properties, especially in light of recent developments in electronics and materials that could help to ease some of the difficulties encountered in the past.

Beyond the aggressive nature of the materials themselves, the difficulties in measuring the thermal conductivity of molten salts are mainly associated with: (1) the high temperatures at which these materials are to be employed; (2) their electrically conducting nature, which presents a particular challenge to some conventional measurement approaches. Specifically, with regards to the first point, the high temperatures make it difficult to maintain a uniform temperature distribution throughout the volume of the tested material in the measurement cell. A non-uniform temperature distribution gives rise to the occurrence of natural convection in the sample, while at high temperatures radiation also plays a non-negligible part in the overall heat transfer. To measure the thermal conductivity it is necessary to isolate the diffusion-driven thermal transfer mechanism from convection and radiation; the presence of strong convention and radiation introduces a difficulty in decoupling the conductive mode of heat transfer and poses additional difficulties for the experimentalist.

The transient hot-wire method has proven to be successful in eliminating the errors arising from natural convection [3] and radiation [4], and therefore is a promising technique for high-temperature measurements. The method

involves electrically heating a metallic wire immersed in a sample and monitoring its change in temperature over time. This technique is, however, not directly transferrable to molten salts in its standard implementation due to the finite electrical conductivity of the salt, which allows part of the current flowing through the wire to leak inside the liquid sample, thus distorting the signal and invalidating the standard analytical model. Specifically, the electrical power dissipated in the wire, and used as a direct indication of the heat deposited in the sample from the wire, is now unknown. One way to avoid current leakage into the sample is to electrically insulate the wire from the sample. Ceramic-coated wires have been used successfully in the past to overcome this problem, e.g. by Alloush et al. [5] and Nakamura et al. [6]; however, the probes used in this approach have the disadvantage of being prone to cracks at high temperature due to the differential expansion between the (thin) ceramic insulating sheath and the internal heated wire, consequently losing their electrically insulating properties.

As an alternative to the ceramic-coated transient hot-wire probe, Omotani et al. used a liquid-metal-filled capillary [7]. The liquid metal can expand freely within the capillary, thus avoiding the aforementioned thermally induced stresses. The authors measured successfully the thermal conductivity of some eutectic nitrates up to 584 K. Subsequently, DiGuilio et al. [8] further explored the idea of Omotani and co-workers by using two Gallium-filled capillaries with a repeatibility less than 1%. Nevertheless, the authors noticed that the technique stopped giving reliable results at around 600 K, and ascribed this observation to the possible decrease in the electrically insulating properties of the quartz at high temperatures.

The main aim of the present work is to further extend the range of applicability of the liquid-metal-filled capillary technique while still maintaining an acceptable level of accuracy. The probe developed here consists of a flexible U-shaped quartz-capillary filled with molten Galinstan. The salt selected to test the proposed probe is the eutectic mixture $KNO_3{-}NaNO_3{-}NaNO_2$, also known as heat-transfer salt (HTS). Its wide liquid-state range of temperatures allows a critical analysis of the probe's performance to be conducted. Further, even if the agreement in the literature regarding the thermal conductivity of HTS is more satisfactory than other salts, there remain some discrepancies that new data can help resolve.

2. Apparatus

The experimental apparatus developed in the present work for the purpose of providing the desired thermal conductivity data consists of three main parts: (1) a furnace; (2) a measurement cell containing the material sample to be tested and the capillary probe; and (3) the electrical circuit with the furnace controls and the data acquisition unit (DAQ).

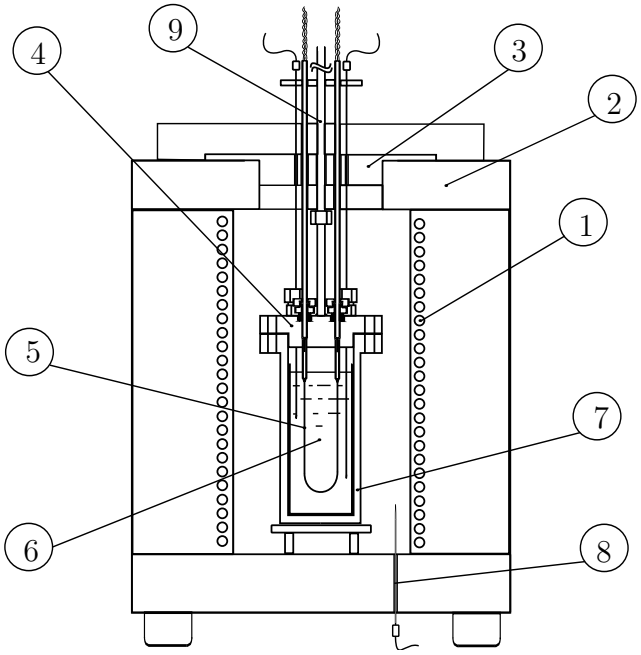

Fig. 1: Furnace schematic, showing: (1) heating elements, (2) insulation, (3) tap, (4) probe support, (5) quartz capillary, (6) specimen (tested material sample), (7) sample container, (8) external thermocouple, and (9) lifting rod

The furnace used is an in-house customisation of a Horbach furnace specifically modified to achieve a temperature distribution inside the sample which is as uniform as possible. A sketch of the furnace is provided in Fig. 1. It comprises a heating cavity with an internal diameter of approximately 100 mm, closed at the bottom, and a 70 mm aperture at the top. During the experiments the cell is inserted into the cavity and the aperture is closed in order to minimise heat losses. The cell is placed at a slight elevation above the bottom of the furnace to facilitate natural convection around the cell and assure a uniform heating of the cell's surfaces. The heating elements

in the furnace are positioned on the side walls of the cavity and are protected by insulating material. A thermocouple is inserted at the bottom to monitor the temperature inside the cavity and for the purpose of avoiding overheating. The furnace is controlled from a computer using as feedback input the temperature measurement inside the cell, measured by a K-type thermocouple.

A schematic of the measurement cell employed in conjunction with the furnace described above is depicted in Fig. 2. The cell is constructed using stainless steel and was designed to have enough thermal mass to smooth the thermal fluctuations inside the furnace. The cell consists of a sample container of internal diameter 41 mm and length 77 mm, and a lid. The volume of material sample needed to conduct a single experimental run is approximately $60-70$ mL depending on the thermal expansion coefficient of the material. The lid is constructed from a stainless steel flange and acts to provide both structural support for the sensing element and the possibility of hermetically sealing the sample container for the case of high-pressure measurements, if these are required. The lid can be raised and lowered by means of a supporting rod, and is equipped with four sealed pressure fittings for inserting temperature sensors and gas connections. In the standard arrangement, one resistance temperature detector (RTD) and two K-type thermocouples are used to measure the temperature and its temporal variation, respectively. Two quartz tubes are inserted into the lid and provide the connection to the Galinstan-filled capillary. Tungsten-rod electrodes are inserted at the end of the quartz tubes and serve as electrical contacts. Each Tungsten rod is laser-welded to two Constantan wires, and connected to the DAQ unit. The Constantan wires are inserted through two double-core alumina rods for electrical insulation. The alumina rods are connected to the lid using standard pressure fittings.

The sensing element consists of a U-shaped quartz-capillary filled with liquid Galinstan. The capillary has internal and external diameters of 0.05 mm and 0.08 mm, respectively. It is connected to two quartz tubes, one on each side, which have an internal diameter of 1 mm. The distance between the two quartz tubes in the arrangement shown in Fig. 2 is 25 mm, and the connections between each tube and the ends of the quartz capillary are made by using high-temperature glue. The choice of using a bent capillary instead of using a straight one was mostly made for practical reasons. A U-shaped capillary decreases the volume of the sample needed; this in turn allows us to minimise heat losses from the arrangement, which achieves a more uniform

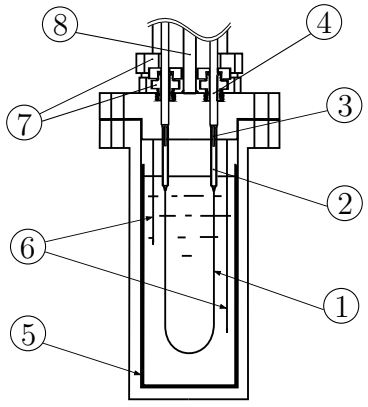

Fig. 2: Cell schematic, showing: (1) quartz capillary, (2) quartz-tube end-connectors and supports, (3) tungsten rod, (4) alumina rod, (5) tested material sample container, (6) thermocouples, (7) pressure fittings, and (8) lifting rod

temperature distribution. In addition, the capillary is more easily replaceable compared to a straight arrangement.

The procedure of forming the capillary into the required form is as follows. Firstly, a quartz capillary (CM scientific) of total length 20 cm is allowed to dry in an oven at 300 °C for 2 h. This procedure is essential in eliminating the moisture present in the capillary; any residual moisture will evaporate at high temperature forming vapour bubbles and interrupting the electrical contacts. Liquid Galinstan is then injected into the capillary through a fine syringe. Paraffin wax is used to seal the syringe needle onto the capillary. The capillary is then cut into a length of approximately $100 - 140$ mm and its length measured. The capillary is then bent in a U-shape and each of its two ends is inserted into a quartz tube, which have been pre-filled with liquid Galinstan. Surface tension assists in creating a good contact between the capillary and the tubes and in avoiding liquid metal spillage. The tubes and the capillary are subsequently sealed by using a combination of high temperature glues (Ceramabond 618-N, Silcoset 158). This operation is the most critical as an accurate and neat sealing has to be achieved in order to electrically insulate the liquid Galinstan without increasing the end effects of the probe (see Section 3.3 for details). The glue is cured, first at 150 °C and then 300 °C. The quartz capillary is then tested at high temperature by briefly heating the capillary with a natural gas flame until the quartz glows; its resistance is monitored at the same time to check for abnormal

behaviour. The capillary is then heated to the softening point of quartz to form the shape depicted in Fig. 2.

The most critical operation is the application of the high temperature glue. This operation is tedious and often causes the capillary to fail halfway through the experiment. To avoid such a failure it was found, by trial and error, that it is absolutely crucial that no air bubbles are retrained within the sealing. These air bubbles interrupt the electrical contacts at the higher temperatures due to thermal expansion. The application of the glues once the liquid Galinstan is already inside the capillary minimises the formation of air bubbles and assures a more uniform spreading and sealing of the glue.

A schematic of the employed electrical circuit is depicted in Fig. 3. The data acquisition sequence starts when the temperature drift with time, as monitored through the thermocouple inside the cell, falls below 0.1 K/min. The DAQ modules NI-9213 and NI-9237 are then used to acquire continuously the signal from the thermocouples and RTDs, respectively. A Wheatstone bridge is used to measure the varying resistance of the capillary during the measurements. The bridge comprises two highly precise resistors (R_2, R_3) and a potentiometer (R_1) to manually balance the bridge during an experiment. The nominal value of R_2 is 100 $\Omega \pm 0.01\%$. R_3 is composed by multiple accurate 1 Ω resistors with very low resistivity temperature coefficients in an arrangement featuring series and parallel connections. This particular arrangement is adopted to minimise the error due to Joule heating in R_3, which was found to be as high as 3% if standard resistors of the same resistance were used. The bridge is powered by a Tektronix PWS 4205 DC power supply. A MOSFET transistor operated from the I/O port closes and opens the circuit. The switching time of the circuit has been measured and found to be less than 2 ms. The voltage across the Wheatstone bridge (V_{AC}) is measured by a NI-9237 DAQ module at a sampling rate of 2 kS/s. With certain adaptations the 50 Hz (background mains noise injected into the electronics) component was removed, and the noise reduced to approximately 4 μV. Voltages are measured at Points B, D and E using a dedicated NI-9239 DAQ module. Manual switches (not shown in Fig. 3) are used to swap between the present circuit and a secondary circuit that is connected to two Keithley 199 DMM digital multimeters. In this way it is possible to measure each resistance in the circuit with at least 1% expanded uncertainty during the experiments and minimise the effect of temperature variations.

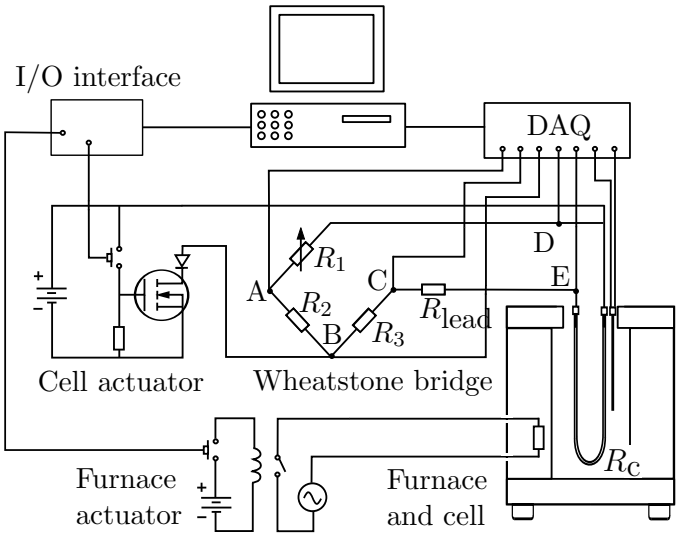

Fig. 3: Schematic of the implemented electrical circuit. The data acquisition sequence and the furnace are both controlled from the I/O interface

3. Experimental Methods

3.1. Measurement basis

The thermal conductivity of the sample (liquid) material is found by modelling the electrically heated probe as a perfect line source (of infinite length and infinitesimal diameter), resting in a stagnant (i.e. stationary) liquid domain (of infinite extent). The working equation for this ideal case was derived by Carslaw and Jaeger [9] by solving the unsteady one-dimensional (1-D) thermal-diffusion equation in a cylindrical-polar coordinate system. The solution describes the increase in temperature of the liquid, ΔT, as a function of time t and the thermal power input per unit length $\dot{q}'$:

$$\Delta T = \frac{\dot{q}'}{4\pi\lambda} \ln\left(\frac{4\alpha t}{r^2 C}\right). \tag{1}$$

In this expression, λ and $\alpha = \lambda/(\rho c_p)$ are respectively the thermal conductivity and the thermal diffusivity of the liquid, r is the radial coordinate as measured from the centreline of the line source, and C is a constant whose natural logarithm is equal to Euler's constant. The equation is valid when the value of $r^2/\lambda t$ is small (i.e. $\ll 1$); a condition easily respected during the

experiments.

Equation 1 can be rearranged and differentiated to find the value of the thermal conductivity of the liquid:

$$\lambda = \frac{\dot{q}'}{(4\pi)} \frac{1}{\mathrm{d}(\Delta T)/\mathrm{d}(\ln(t))} \,. \tag{2}$$

When applied to the quartz-capillary arrangement used in this work, Eq. 2 relates the thermal conductivity of the liquid sample to the rise in the temperature of the capillary caused by a thermal input originated by imposing a known electrical power to the capillary probe. The temperature rise of the capillary during an experiment is calculated as:

$$\Delta T = \frac{\Delta R_{\mathrm{C}}}{\mathrm{d}R_{\mathrm{C}}/\mathrm{d}T} \,, \tag{3}$$

where R_{C} is the resistance of the capillary as measured by the Wheatstone bridge and $\mathrm{d}R_{\mathrm{C}}/\mathrm{d}T$ is its dependence on the temperature. The measured temperature rise of the capillary during the experiments reported in this paper was found to be between 3 and 7 K, depending on the applied power.

The resistance of the capillary R_{C} is calculated from the voltage measured across the Wheatstone bridge, V_{AE}:

$$R_{\mathrm{C}} = \frac{(R_3 + R_{\mathrm{lead}})\left[R_1 + (R_1 + R_2)\frac{V_{\mathrm{AE}}}{V_{\mathrm{BD}}}\right]}{R_2 - (R_1 + R_2)\frac{V_{\mathrm{AE}}}{V_{\mathrm{BD}}}} \,; \tag{4}$$

where the constants R_1, R_2, R_3 and R_{lead} are the resistances described in Fig. 3 and are approximately constant during one measurement while V_{BD} is the voltage applied to the bridge.

Based on the knowledge of the capillary resistance R_{C}, the value of the derivative term $\mathrm{d}R_{\mathrm{C}}/\mathrm{d}T$ can be found by plotting the probe resistance R_{C} as a function of temperature and fitting a linear relationship to the data. A typical plot of the residuals from such a linear fitting is shown in Fig. 4 for a probe with a resistance of approximately 15 Ω (and a $\mathrm{d}R_{\mathrm{C}}/\mathrm{d}T$ value of 0.0122 Ω/K). As indicated by the figure the residuals are uniformly scattered over the temperature range, suggesting that a linear relationship is a reasonable fit to the data, and by extension, that the extracted (constant) value of the derivative $\mathrm{d}R_{\mathrm{C}}/\mathrm{d}T$ is an accurate measurement of this term.

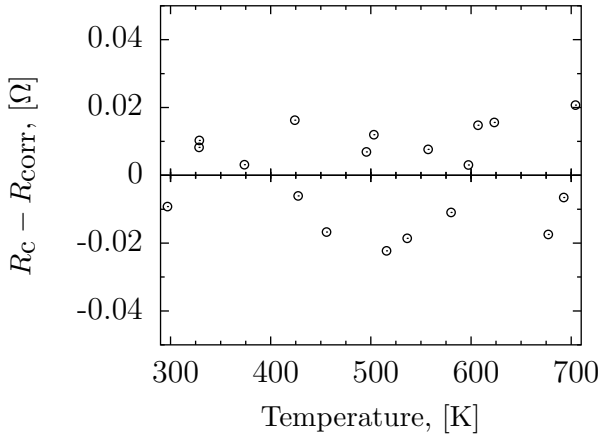

Fig. 4: Residuals of a linear fit to the capillary resistance versus temperature data. The uniform distribution of the residuals indicates a constant value of $\mathrm{d}R_c/\mathrm{d}T$

Furthermore, the total power $\dot{Q}$ dissipated in the capillary is found by measuring the current I passing through the capillary:

$$\dot{Q} = R_c I^2 \,. \tag{5}$$

The current is calculated from the voltage drop V_{BC} across resistance R_3. The thermal power $\dot{Q}$ was confirmed as varying only slightly during each measurement run; its average value during each run is used. The power input per unit length $\dot{q}'$ is then calculated by dividing $\dot{Q}$ by the length of the capillary. At this point all terms needed to evaluate the thermal conductivity of the liquid sample λ from Eq. 2 are, in principle, known.

Nevertheless, because of inevitable imperfections and end-effects in the connections between the capillary and the supporting quartz tubes, it is impossible to establish exactly the effective length of the capillary exposed to the fluid. In a series of tests, the actual length of the capillary was used to calculate λ for known liquids (see Section 3.2), and it was found that all measurements suffered from a systematic error of $6-10\%$ depending on the probe. It was therefore decided to adopt the same procedure described by Hoshi et al. [10], and to use an effective length l_e for calculating $\dot{q}'$:

$$\dot{q}' = \frac{\dot{Q}}{l_\mathrm{e}}\,. \tag{6}$$

The effective length was estimated via an additional set of calibration runs with known (standard) fluids (Section 3.2).

3.2. Testing and calibration

The effective length l_e was calculated by matching the measured thermal conductivity of DI water at ambient temperature with its reference value. DI water was chosen as the calibration fluid because its thermal conductivity is similar to that of HTS. A water bath was used to ensure a uniform temperature distribution during the calibration measurements. The calibrated probe, along with the established effective length l_e from the DI water runs was then further tested against Toluene and Glycerol at elevated temperatures up to 430 K. All the calibrated probes measured the thermal conductivity of Toluene and Glycerol with an error less than 2%. Typical results from the calibration tests are shown in Table 1.

Table 1: Test measurements of the current probe against reference data for DI water, Toluene and Glycerol, taken respectively from Ramires et al. [11, 12] and CINDAS [13].

Liquid	**Temp. [K]**	**λ (meas.) [W/m K]**	**λ (ref.) [W/m K]**	**Error [%]**
DI Water	305.5	Calib. Ref.	0.6184	–
	331.1	0.6495	0.6509	-0.2
Toluene	276.2	0.1367	0.1376	-0.7
Glycerol	301.7	0.2903	0.2855	1.7
	326.9	0.2923	0.2886	1.3
	374.6	0.2974	0.2948	0.9
	431.2	0.3028	0.3022	0.2

3.3. Method performance and measurement uncertainty

A complete analysis of the performance of the present method is possible up to 430 K by comparing the measurement results of standard fluids with their relatively accurate literature data. In this range, the precision of

the method was quantified by the expanded deviation of repeated measurements, given a 95% confidence interval. The expanded deviation was found to increase slightly with temperature and to reach a value of 0.8% at 430 K. The dominant effect acting to limit precision is attributed to the presence of non-negligible natural convection in the fluid volume inside the cell. It was indeed noticed that when the temperature gradient in the cell was higher, the repeatability decreased. The trueness of the method, as calculated by the maximum difference between the mean of repeated measurements of standard fluids and their reference data, was less than 2%. Considering that the thermal conductivity of the liquids used as a reference is also known within an error, a 2% trueness is considered adequate for measurements up to 430 K. Major sources of bias can reside in the non-negligible natural convection in the fluid, in the end effects, and in the non-straight arrangement of the capillary. Above 430 K the precision of the method remained at around 1% until $680 - 700$ K. Above this temperature the repeatability of the measurements gradually deteriorated, owing to a failure of the connections between the capillary and the quartz support-tubes at high temperatures. Specifically, it was found that these connections had the propensity to crack above 700 K, which led eventually to the failure of the electrical insulation between the liquid Galinstan inside the probe and the salt in the surrounding container. The authors are confident that this failure can be resolved if measurements at temperatures higher than 700 K are necessary; however, the present data were considered adequate for the purposes of the present study.

The combined expanded uncertainty (95% confidence interval) of the thermal conductivity data of HTS presented in this study was calculated from the expanded uncertainty in the calculated value of the thermal conductivity and the expanded uncertainty in the drift from the true value caused by systematic errors. The expanded uncertainty in the calculated thermal conductivity was derived from the uncertainties of the measured quantities using Eq.2, and found to be 1.3%. The major component of the uncertainty in the calculated thermal conductivity was found to arise from the term $\mathrm{d}\Delta T/\mathrm{d}\ln(t)$. It is important to note that any errors in the evaluation of the temperature dependence of the capillary resistance, $\mathrm{d}R_\mathrm{c}/\mathrm{d}T$, are embed in l_e and thus need not be considered independently.

The expanded uncertainty in the drift between the calculated and true value of thermal conductivity was evaluated by taking into account the systematic errors affecting the measurements below 430 K and other possible systematic errors arising at high temperature. The expanded uncertainty in

the drift caused by the first group was considered equal to the maximum drift found when measuring standard fluids (equal to 2%). Regarding the second group, the only added major source of systematic error that we could identify at higher temperature was radiation.

Insightful studies into the effect of radiation were conducted by Menashe et al. [14] and Nieto De Castro et al. [4]. Nieto De Castro et al., in particular, showed that the error due to radiation in the transient hot-wire method could account for more than 3% of the total error. The effect of radiation induces a concave curvature in the plot of $\mathrm{d}\Delta T/\mathrm{d}\ln(t)$. In some of our measurements we indeed noticed a slight concave curvature. However the curvature was not pronounced and was difficult to detect, probably owing to the lower quality of the data and the different absorptivity of the salt. As a consequence, the analysis of Nieto De Castro et al. is difficult to apply to our study; a preliminary correction over those plots where the curvature was more visible indicated a maximum deviation of less than 0.7% from the present results. The expanded uncertainty caused by radiation was considered equal to this maximum deviation. The combined expanded uncertainty (95% confidence interval) of the present measurements was then calculated from the expanded uncertainty in the calculated value of the thermal conductivity, the expanded uncertainty in the drift from the true value found below 430 K, and the expanded uncertainty caused by radiation. Based on these values, the combined expanded uncertainty was found to be 3.1%.

The present analysis did not use some of the corrections generally adopted in the standard transient hot wire method to account for non-ideal effects such as the finite radial dimension of the wire or the presence of an insulating layer (see, for example, Menashe et al. [14]). These corrections are normally employed to achieve standard measurement uncertainties lower than 1%. Because the standard uncertainty in the present study is higher than this, the magnitude of these corrections was found to be not significant and therefore they were not included. In addition, in the standard transient hot wire method a pair of long and short wires are normally used in the attempt to account for the end effects of the wire, by subtracting their respective outputs. This method effectively reduces the end effects under many different experimental conditions (power input, type of fluid, etc.). Indeed any variation in the magnitude of the end effects caused by the mentioned conditions will affect the short and long wire in the same manner and therefore they are eliminated by subtracting the wire outputs. On the other hand, the use of an effective capillary length cannot completely account for end effects which

are very different than the ones for which the probe was calibrated. The use of an effective length therefore results in a higher systematic error compared to the use of a short and long wire. Future work will investigate the use of a short and long capillary.

It is important to discuss briefly the role of the not-straight arrangement of the capillary. This particular arrangement could affect the accuracy of the measurements in three ways: (1) the working equations for the transient hot-wire method do not rigorously apply; (2) the non-vertical alignment decreases the time for the onset of natural convection; and (3) the non-vertical alignment magnifies the error due to natural convection already present is the cell.

With respect to the first issue, we found that Eq. 1 could predict satisfactory the behaviour of fluids of known thermal conductivity, and the linearity of $\mathrm{d}\Delta T/\mathrm{d}(\ln(t))$ was conserved. This is not unexpected if we consider that the diffusive heat transfer length scale λ_d is approximately defined as:

$$\lambda_\mathrm{d} = \sqrt{\alpha\tau}\,, \tag{7}$$

where α is the thermal diffusivity of the liquid and τ the timescale of the measurement. If we take 5×10^{-7} m^2/s and 1 s as conservative values for respectively α and τ, λ_d is approximately 0.7 mm, much less than the overall length of the capillary (about 100 mm).

With respect to the onset of natural convection, we found that this occurs between 0.6 and 1.6 s, that is indeed less than what is usually encountered by using a straight capillary. However the time window is always wide enough to assure an accurate calculation of $\mathrm{d}\Delta T/\mathrm{d}(\ln(t))$ and the aforementioned effect does not undermine the measurement.

Finally, the non-vertical alignment of the capillary would likely cause the diffusion of heat to be parallel to the flow direction and consequently modify the ideal temperature field. To avoid this effect the temperature distribution inside the container is kept as homogenous as possible and the temperature gradient during a measurement is always less than the differential error between the thermocouples (<0.3 K). Even with this precaution, natural convection could occur with a temperature difference less than 0.3 K and indeed part of the current error could be ascribed to the non-vertical alignment of the capillary.

3.4. Materials and procedure

HTS has been selected as the material of interest in the present study, because its melting point is within the range of temperatures for which the thermal conductivity of standard fluids such as Glycerol can be measured by the developed approach. In this way, the performance of the probe can be ascertained by allowing a smooth transition between the experimental conditions used for conducting the measurements of standard fluids and the ones used for HTS.

HTS was obtained by mixing KNO_3, $NaNO_3$ and NO_2 at a respective molar-ratio of 0.44:0.07:0.49. All salts were in powder form with at least 99% purity. The quantity of each salt was weighed using a laboratory scale with an uncertainty of $\pm\,0.01$ g. The salts were firstly mixed well, and then melted in a sample container. The high porosity of the powder caused the volume of the salt to decreases as the melting process took place, so that it was necessary to add additional quantities of salt to the container in order to reach the level of liquid required for the measurements. Once the sample container was filled with liquid salt, the probe was lowered and immersed into the liquid. The furnace was closed and insulated, and the temperature left to stabilise based on a specified set-point and also until any temporal temperature variations, as measured by a 1 mm-thick reference thermocouple, dropped below 0.1 K/min. This took approximately one hour. The bridge was then balanced using a current pulse and the data acquisition sequence started. The measurements were repeated with at least two different power inputs, with at least two repetitions per test. Having completed a test at one temperature, the temperature was then changed and the procedure repeated. During the measurements, the temperature range was swept back and forth to avoid any change in the capillary behaviour with thermal aging, and in order to quantify the presence of any hysteresis in the results. Three different probes were used to measure the thermal conductivity of HTS.

Once the data acquisition sequence is initiated, the NI 9237 module commences data logging from the Wheatstone bridge and, subsequently, the I/O interface closes the bridge circuit described in Fig. 3. The voltage across the bridge is measured at a typical sampling rate of 2 kS/s and converted to a temperature rise according to the aforementioned expression; a typical plot of the temperature rise is depicted in Fig. 5. The value of $\mathrm{d}(\Delta T)/\mathrm{d}(\ln(t))$ is calculated from linear fitting to the temperature rise versus (logarithmic) time curve. Fig. 6 shows the relative residuals of such fitting. The temperature was found to increase linearly with $\ln(t)$ at least between 0.15 and

0.6 s. Before 0.15 s the theoretical model was not applicable due to second order unsteady effects caused by the finite dimensions of the capillary [15]. After 0.6 s, depending on the properties of the sample and the temperature distribution in the cell, natural convection occurred and the rate of rise in the temperature of the capillary diminished. The start of natural convection could be easily detected because the residuals of linear fittings increased drastically. In some cases, convection was found to occur as late as 1.6 s from the start of the measurement.

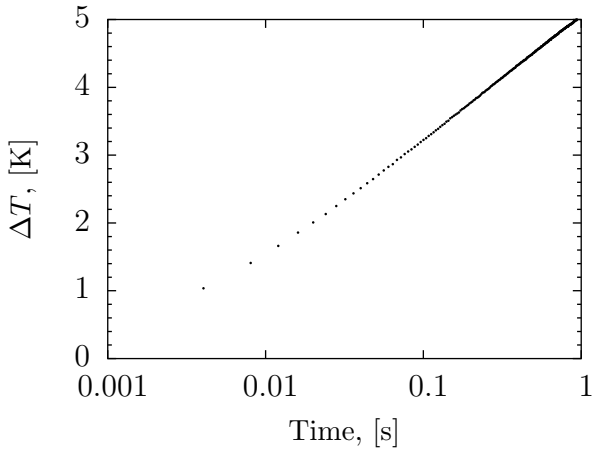

Fig. 5: Temperature rise of the capillary as a function of time. The mathematical model for transient hot wire method applied to the U-shaped capillary

4. Results and Discussion

The results of the thermal conductivity measurements for HTS are shown in Fig. 7 along with data found in the literature. In addition, we report the data in Table 2, in particular the mean value of the measurements and their standard deviation over an interval of ± 10 K. The current data agree well with those of Tufeu et al. [16] who used a concentric-cylinder, steady-state method. Omotani et al. [7] used a method similar to the present one with a claimed accuracy of 3% [7]. Their data fall approximately 3.5% lower than ours. Considering that the difference between these studies is approximately equal to their respective claimed accuracies, the agreement is more than acceptable.

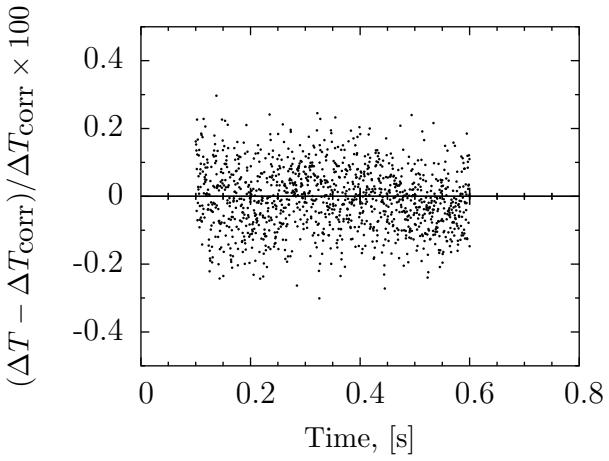

Fig. 6: Relative residuals of the linear fitting of the temperature rise versus $\ln(t)$. The uniform distribution of the residuals indicates a linear increase of $\ln(t)$ with time

The results of Odawara et al. [17] lie approximately 8% higher than the current measurements. Odawara et al. [17] used an optical method to measure the thermal conductivity of molten HTS and $NaNO_3$. In his study the thermal conductivity was derived indirectly from the thermal diffusivity of the salt, and it is possible that this inference introduced a further uncertainty into the resulting data. It is worth noting that the results of Odawara et al. [17] with respect to $NaNO_3$ are also higher (by approximately 10%) than the generally accepted values of Kitade et al. [21], as discussed by Nagasaka et al. [22].

The results of Cooke [18] at relatively low temperatures are very close to those in the present study, while the two studies due show deviations at higher temperatures. To further understand this discrepancy, we carefully reviewed the work done by Cooke. Fortunately the author reported in detail and with very good precision all the measurements, including raw data [18]. Cooke used a variable-gap apparatus consisting of two parallel heated-plates. The apparatus was used to measure the thermal resistance of the liquid between the two plates at different gaps between the plates. The thermal conductivity was then found by calculating the slope of the thermal resistance versus gap thickness curve. At around 470 K the thermal resistance was found to increase linearly with the thickness of the gap. This allowed for an accurate calculation of the slope, and also suggested that external effects

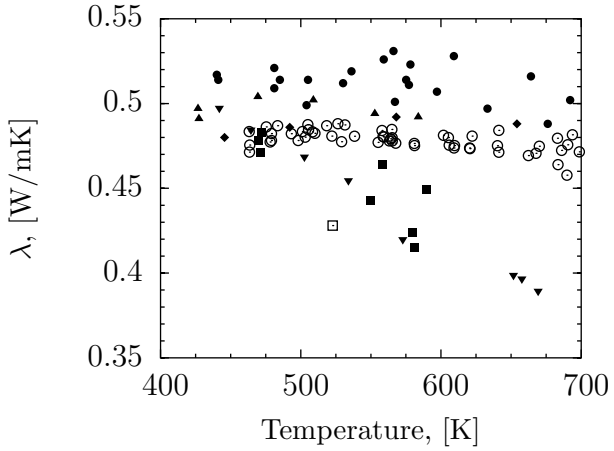

Fig. 7: Thermal conductivity of HTS: (⊙), present study; (⧫), Tufeu et al. [16]; (▲), Omotani et al. [7]; (●), Odawara et al. [17]; (■), Cooke [18]; (▼), Turnbull [19]; (⊡), Vargaftik [20]

were negligible. At higher temperatures, on the other hand, this linearity was lost. This different behaviour is caused by secondary effects such as radiation, natural convection and additional heat losses. To overcome these effects, Cooke calculated the thermal conductivity by extrapolating the slope to zero gap thickness. Indeed when the thickness approaches zero, these secondary effects should be reduced significantly. In practice, however, the author estimated the slope from a linear fitting of the data points obtained using small gaps. By doing this, the number of data points used is much lower than the overall set of data, and the choice concerning which data points to include in this exercise becomes, at least to some extent, subjective. In addition, the relative error in measuring the thickness of the gap increases, as the gap decreases. The net result is a loss of accuracy and a larger scatter, as is visible in Fig. 7. Moreover, it is possible that the aforementioned secondary effects are still non-negligibly present when the gap is small. In our opinion, these are possible reasons that can be used to explain the discrepancy with the current measurements. Nevertheless, Cooke [18] is an excellent effort, and we observed that whenever the linearity was reasonably conserved over the whole data range thanks to the lack of these issues, Cooke's data are in very good agreement with ours.

Turnbull [19] pioneered the application of the transient hot-wire method to molten salts by using a bare metallic wire with no electrical insulation.

Current leakage is highly likely to have affected this measurement, as discussed by Omotani et al. [7]. Omotani et al. [7] also noted how previous measurements conducted by their group [10], and later discarded because of current leakage, led to results similar to the ones of Turnbull.

Furthermore, Vargaftik et al. [20] were the first to measure the thermal conductivity of HTS. Unfortunately, their measurement results seem unreliable because the calibration tests gave different results compared to the most accepted literature values for standard fluids, as discussed by Turnbull [19].

Table 2: Thermal conductivity of HTS at different temperatures along with its mean standard deviation (SD). The data statistics were compiled from a series of experiments/data points over an interval of ± 10 K around each stated temperature.

Temp. [K]	λ [W/m K]	**SD**
471.7	0.479	0.0047
503.1	0.483	0.0026
527.3	0.483	0.0045
562.1	0.480	0.0026
606.4	0.477	0.0029
640.9	0.477	0.0054
666.8	0.471	0.0023
689.3	0.472	0.0078

Proceeding further, we can now propose the following relationship for the variation of the thermal conductivity of molten HTS with temperature:

$$\lambda = 0.382 + 3.85\times10^{-4}\,T - 3.72\times10^{-7}\,T^2 \qquad \text{for} \qquad 460\,\text{K} < T < 700\,\text{K}, \quad (8)$$

where λ is given in W/m K. This relationship was derived from a quadratic fitting to the values reported in Table 2.

It is important to mention that the data seem to suggest a maximum thermal conductivity of about 0.483 W/m K over the approximate range $500\,\text{K} < T < 530\,\text{K}$, a behaviour also evidenced in the data of both Tufeu et al. [16] and Omotani et al. [7], as shown in Fig. 7. However, the deviation caused by such maximum from a simple linear fitting to the data is similar to the present experimental error and it is difficult to state definitively.

It is interesting to calculate the thermal conductivity of HTS as the molar average of the thermal conductivities of its pure constituent components. Unfortunately, only few data are available for $NaNO_2$, and over a limited range of temperatures. If the data of Tufeu et al. [16] are used, the thermal conductivity of HTS over the temperature range between 560 and 600 K (where data for $NaNO_2$ are available) is around 0.480 W/m K, which less than 1% from the reported relationship above. This additive behaviour of the thermal conductivity of molten salts, pointed out in previous studies, e.g. Omotani et al. [7], seems to be confirmed by the present data.

Based on all previous results and the related discussion, the overall performance of the present instrument and technique seem satisfactory. It is rather interesting that the U-shaped capillary is able to give very reasonable results and perform with an accuracy similar to other studies done with a straight capillary [7], which is more representative of the theoretical model. This is a welcome result, which can also help towards a better understanding of the effect of natural convection on the transient hot-wire method. Specifically, it endorses the claim that the effect of natural convection is negligible, as long as the time window over which the measurements are acquired is short enough not to allow the generation of fluid circulation currents in the tested fluid-material. Of course, such short time-windows over which to make these measurements require sensible electronics and low-noise signals, but this is a condition that today is much easier to achieve than in the past. The U-shaped arrangement will probably not be able to achieve the accuracy of the straight transient hot-wire, which has proven to be capable of reaching uncertainties below 1% [8]. However, for its applications in particular systems, such as molten salts, the present overall error of 4% is more than satisfactory and the present method has some practical advantages, such as requiring a smaller sample volume for the measurement.

The capillary probe has proven capable of conducting molten-salt thermal-conductivity measurements with reasonable results up to 700 K. We also conducted some destructive measurements beyond 700 K. The maximum temperature at which we could obtain reliable data was 730 K. After about 700 K, some measurements were found to be erroneous. It was identified that the problem resided in the capillary connections to the supporting quartz-tubes. The connections were found to fail between 700 and 730 K exposing the liquid Galistan to the molten salt or causing the capillary to detach from the support. We believe that this is a problem that can be resolved, allowing measurements at even higher temperatures. Future work will be directed

towards finding a suitable material for making these connections.

Finally, it is useful to discuss briefly the potential problem of current leakage in the present instrument, as identified in the work by DiGiulio et al. [8]. The authors stated that the quartz lost its electrical insulating properties in their experiments at temperatures higher than 590 K. In our case, we did not encounter any sign of current leakage, at least up to 700 K. If current leakage was present in our system the quality of the measurement would decrease substantially due to preferential current path caused by the U-shape configuration. In addition, in some experiments the sample container was polarised compared to the Wheatstone bridge so that a minimal short circuit between the two could have been easily sensed. DiGiulio et al. [8], however, offered convincing arguments that current was leaking through the quartz. As a possible explanation, we may suggest that the different behaviours between the studies could be ascribed to either the quality of the quartz or the higher reactivity of liquid Gallium compared to liquid Galinstan.

5. Conclusion

This study reported on a successful implementation of an instrument and a related technique based on a Galinstan-filled, U-shaped capillary to measure the thermal conductivity of molten HTS up to 700 K (430 °C). The thermal conductivity of HTS was found to range from 0.48 W/m K at 500 K to 0.47 W/m K at close to 700 K, with a reported expanded uncertainty (95% confidence interval) of 3.1%. It was demonstrated that the U-shape capillary can satisfactorily behave as the conventional transient hot-wire method based on an infinite line-source, and, in addition, benefits from some practical advantages. Furthermore, contrary to DiGiulio et al. [8], it was noted that the quartz capillary retains its electrically insulating properties, at least up to 700 K, while with additional modifications it seems possible to extend the operating temperature envelope of the instrument even further. It can be concluded that the present method appears suitable for measuring the thermal conductivity of high temperature fluids, including that of conducting fluids such as molten salts. Moreover, the generated data regarding the thermal conductivity of HTS presented herein were used to elucidate the disagreement in previous literature and to support the linear mixing rule of the thermal conductivity as described by Tufeu et al. [16].

6. Acknowledgments

The authors wish to thank the UK Centre for Nuclear Engineering (UKCNE), and its Director Professor W.E. Lee, for awarding NLB a PhD studentship and financially supporting the project, Professors G.F. Hewitt and W.A. Wakeham for the interesting discussions and useful advises, and Professor A. Nagashima for sharing the details of his probe.

References

[1] V. M. B. Nunes, M. J. V. Lourenço, F. J. V. Santos, C. A. Nieto de Castro, J. Chem. Eng. Data 48 (2003).

[2] X. Zhang, M. Fujii, Int. J. Thermophys. 21 (2000).

[3] J. J. Healy, J. J. De Groot, J. Kestin, Physica B+C 82 (1976).

[4] C. A. N. de Castro, R. Perkins, H. Roder, Int. J. Thermophys. 12 (1991).

[5] A. Alloush, W. B. Gosney, W. A. Wakeham, Int. J. Thermophys. 3 (1982).

[6] S. Nakamura, T. Hibiya, F. Yamamoto, Rev. Sci. Instrum. 59 (1988).

[7] T. Omotani, A. Nagashima, J. Chem. Eng. Data 29 (1984).

[8] R. M. DiGuilio, A. S. Teja, Int. J. Thermophys. 13 (1992).

[9] H. S. Carslaw, J. C. Jaeger, *Heat in Solids*, volume 1, Clarendon Press, Oxford, 1959.

[10] M. Hoshi, T. Omotani, A. Nagashima, Rev. Sci. Instrum. 52 (1981).

[11] M. L. V. Ramires, C. A. N. de Castro, Y. Nagasaka, A. Nagashima, M. J. Assael, W. A. Wakeham, J. Phys. Chem. Ref. Data 24 (1995).

[12] M. L. V. Ramires, C. A. N. de Castro, R. A. Perkins, Y. Nagasaka, A. Nagashima, M. J. Assael, W. A. Wakeham, J. Phys. Chem. Ref. Data 29 (2000).

[13] CINDAS, Properties of Inorganic and Organic Fluids. CINDAS Data Series on Material Properties, volume 1, Hemisphere Publishing Corporation, London, 1988.

[14] J. Menashe, W. Wakeham, Ber. Bunsen Ges. Phys. Chem. 86 (1982).

[15] R. Mathie, C. N. Markides, Int. J. Heat Mass Transfer 56 (2013).

[16] R. Tufeu, J. P. Petitet, L. Denielou, B. Le Neindre, Int. J. Thermophys. 6 (1985).

[17] O. Odawara, I. Okada, K. Kawamura, J. Chem. Eng. Data 22 (1977).

[18] J. W. Cooke, Oak Ridge Nat. Lab. ORNL-4831 (1973).

[19] A. G. Turnbull, Aust. J. Appl. Sci. 12 (1961).

[20] N. B. Vargaftik, B. E. Neimark, O. N. Oleshchuck, Bull. All-Un. PWR Eng. Inst 21 (1952) 1.

[21] S. Kitade, Y. Kobayashi, Y. Nagasaka, A. Nagashima, High Temp. High Pressures 21 (1989).

[22] Y. Nagasaka, A. Nagashima, Int. J. Thermophys. 12 (1991).